ISSN 2250-3153

Tolerance Ring Improvement for Reducing Metal Scratch

Pattaraweerin Woraratsoontorn*, Pitikhate Sooraksa**

* Department of Electrical Engineering, King Mongkut's Institute of Technology Ladkrabang, Thailand
** Department of Information Engineering, King Mongkut's Institute of Technology Ladkrabang, Thailand

Abstract- In hard disk drive manufacturing, the tolerance ring is commonly used for coupling a bearing cartridge to an arm actuator. Further, the tolerance ring can prevent slippage between the arm actuator and bearing assembly during operation of disk drive or during shock events. The metal scratch occurred in the tolerance ring installation process cause a number of particles. The main purpose of this analysis is to improve and to investigate behaviors of the tolerance ring using finite element 3D model for reducing the particles. The result shows that the developed vulnerable point effect less movement of the tolerance ring, the particles were decreased because the metal scratch was eliminated.

Index Terms- Tolerance Ring, Finite Element, Bearing

I. INTRODUCTION

In the hard disk drive (HDD) manufacturing, the present tolerance ring (T-Ring) assembly relates to method, in disk drive to couple actuator arm to bearing assembly. Further, tolerance ring can prevent slippage between the arm and bearing assembly during operation of disk drive or during shock events. Some tolerance ring designs and installation methods include ring with protrusions that frictionally engage with an inner surface of an actuator arm. This ring can be installed by first installing the ring into an actuator arm and then forcibly pressing a bearing assembly into the ring—a press fit where an inner diameter of the ring is smaller than an outer diameter of the bearing assembly. Conversely, rings can first be installed around the bearing and then forcibly pressed into the actuator arm—a press fit where an outer diameter of the ring's protrusions is larger than an inner diameter of the actuator arm. Either way, the act of forcibly pressing a component into another component creates particles as surfaces scratch against each other, particularly when a metal surface is involved.

Many researchers have studied the characteristics of the tolerance ring. Rongley [1] developed a tolerance ring by having a plurality of corrugations of different heights to provide different available spring rates even if one or more of the corrugations of one height is crushed. Cramer, Jr. et al.[2] improved the tolerance rings with permitting them to be utilized in holding cylindrical members within sheet panels and providing positive axial retention of the ring in the sheet panel. The formation of shoulders on the engaged members was not required, but rather through the use of an annular split ring shim. Misso et al.[3] attempted reducing manufacturing cost and increasing disk drive actuator assembly stiffness. A post extends from a base deck and supports an actuator assembly and cartridge bearing. Macpherson et al.[4] increased frictional coefficient between the cartridge sleeve and ring prevents slip between them, eliminating the need to increase compressive forces between the ring and bore and bearing. Piriyakorn and Sujin[5] studied the tolerance ring installation process using finite element 3D model. Although the tolerance ring has been being developed, design one for reducing the particles has never been mentioned. The main purpose of this analysis is to improve and to investigate behaviors of the tolerance ring composed in hard disk drive using finite element 3D model for reducing the particles. Figure 1 shows the actual tolerance ring in hard disk drive.

Figure 1: T-Ring in hard disk drive

II. GOVERNING EQUATION

The finite element simulation of the tolerance ring installation process has been performed with ANSYS LS-DYNA the commercial software package [6].

For linear elasticity, stress given by Hook's law

$$\dot{\sigma}_i = \lambda\left(\frac{\dot{V}}{V}\right) + 2G\dot{\varepsilon}_i \tag{1}$$

i = 1, 2, 3,… where λ is Lame's constant and G is known as shear modulus

The principal stresses (σ_i) can be decomposed into a hydrostatic and a deviatoric component

$$\sigma_i = -P + s_i \tag{2}$$

$$P = -\frac{1}{3}\left(\sigma_1 + \sigma_2 + \sigma_3\right) \tag{3}$$

Where P is the pressure and s_i are stress deviators then

$$P = K\left(\frac{\rho}{\rho_0} - 1\right) \tag{4}$$

$$ds_i = 2G\left(d\varepsilon_i - \frac{dV}{3V}\right) \tag{5}$$

The explicit dynamics simulation, the equilibrium equations in dynamic analysis can be written in the form

$$[M]\left[\ddot{u}^{(i)}\right] = \left[F^{(i)}\right] - \left[I^{(i)}\right] \tag{6}$$

where [M] is mass matrix, F is the vector of externally applied load and I is the vector of inertia forces. The mathematically equilibrium relation is a system of linear differential equations of second order. The solution can be obtained by finite difference expression to approximate the accelerations and velocities in terms of displacement which can be written as

$$\ddot{u}^{(i)} = \frac{1}{\Delta t^2}\left(u^{(i+1)} - 2u^{(i)} + u^{(i-1)}\right) \tag{7}$$

The error of calculation depends on stable increment of time as the relation is shown below

$$\Delta t_{stable} = \min\left(\frac{L_c}{c}\right) \tag{8}$$

where L_c is limited element edge length and c is velocity of longitudinal wave for an element is in the form

$$c = \sqrt{\frac{\lambda + 2\mu}{\rho}} \tag{9}$$

λ and μ is Lame' constants can be written in terms of young's modulus and passion ratio as follows

$$\lambda = \frac{\upsilon E}{(1+\upsilon)(1-2\upsilon)} \tag{10}$$

$$\mu = \frac{E}{2(1+\upsilon)} \tag{11}$$

The stable time expression mentioned for only one element in practically the LS-DYNA solver automatically calculates the minimum time step for each element based on its characteristic length and density. The smallest of these element time steps is called the critical time step. The actual time step used during solution is the product of the current critical time step and a stability factor (usually 0.90). As elements distort during the analysis, their time steps are recalculated. However, an element's time step is calculated based on its material properties (E,υ,ρ) and characteristic length. The equation can be rearranged to find the required density of each element for a desired time step size. By adding the corresponding mass to these elements, the solution time will be reduced. This procedure is known as mass scaling and not recommended. In this simulation, mass was not added to speed up run. A three-dimensional (3D) and a cross-sectional view of the finite element (FE) model used for the tolerance ring installation process are shown in Figure 2.

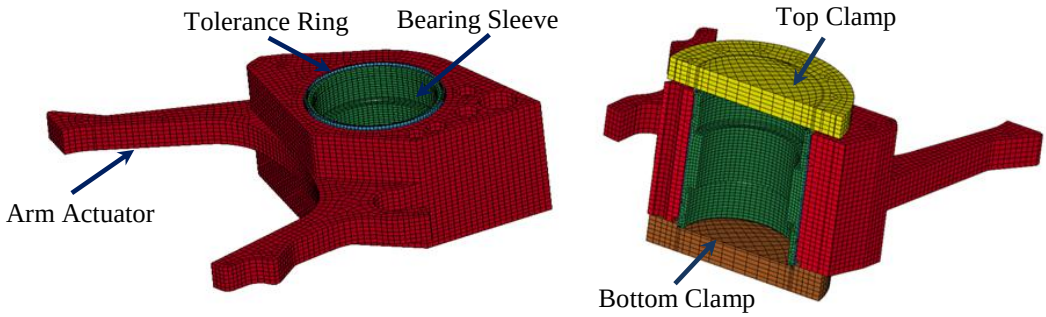

Figure 2: (a) Three-dimensional (3D) model and (b) Cross-sectional view of the finite element (FE) model used for the tolerance ring installation process

Figure 3 shows the concept of the bearing push out after the ring collapsed. The equation of bearing push out can be derived from

$$F = \mu N \tag{12}$$

$$N = VM \times A \tag{13}$$

Where VM is Von Mises Stress

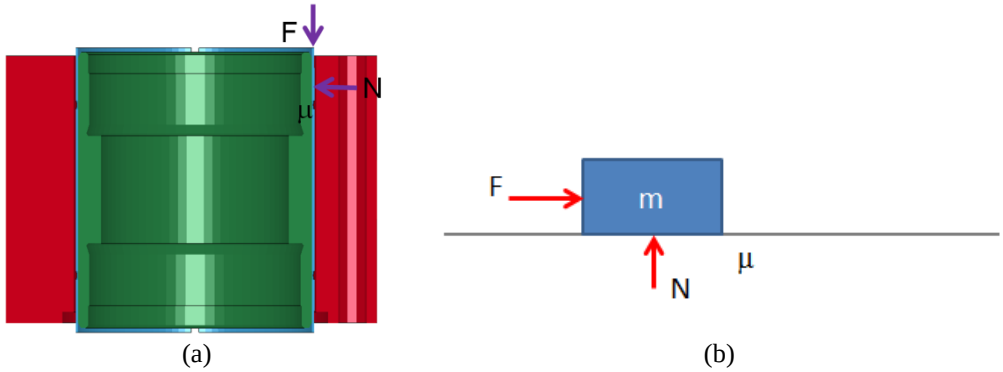

Figure 3: (a) Free body diagram of bearing push out (b) Equivalent system of bearing push out

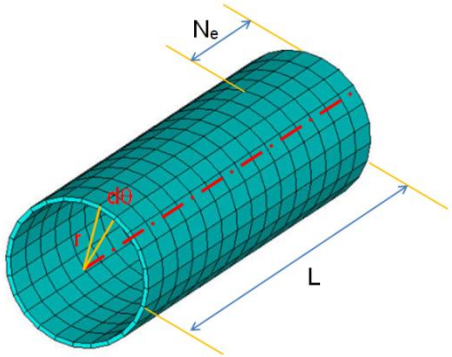

Figure 4: Configuration of cylindrical for finite element model

A bearing sleeve was meshed by control layer of the element as show in Figure 4.

and now substitution eq. (13) into eq. (12) got

$$P_{force} = r\mu \int_0^{2\pi} F \frac{rL}{N_e} d\theta \tag{14}$$

Simplify the eq. (14) obtain

$$P_{force} = \mu F A \frac{D}{2N_e} \quad (15)$$

where P_{force} is bearing push out, μ is coefficient of friction, F is contact pressure, D is a diameter of the bearing sleeve, and N_e is the number of engaged element. Practically, an average pressure and contact area substitution in eq. (15) to obtain bearing push out.

III. FINITE ELEMENT MODEL DESCRIPTION

In this study, the three dimensions and behaviour of the tolerance ring was studied. A space between the arm actuator and the bearing sleeve was determined for collapse of tolerance ring. In addition, the optimal vulnerable points for collapse of the tolerance ring were evaluated as shown in Figure 5. The geometrical model of the tolerance ring has been finalized from native SolidWorks CAD3D commercial software. ANSYS LS-DYNA generated mesh and solved the numerical model. A three-dimensional (3D) finite element (FE) model of tolerance ring showed in Figure 2 composed of 381,190 elements and 54,293 nodes. The ring element has been defined high density to achieve realistic behaviour during collapse. The tolerance ring assembly considered in this study consists of five main components i.e. E-block arm (Arm actuator), bearing sleeve, tolerance ring and two clamps (top and bottom clamp). The E-block arm was simplified with regardless the root arm to reduce amount of element. The bearing cartridge was considered as bearing sleeve that makes sense. The both clamps were considered to be rigid body, the bottom clamp was fixed all degree of freedom as for the top clamp can be moved down in z-direction only via load curve. All components were contacted together by surface to surface. Mechanical properties of different components of FE model are shown in Table 1. Coefficient of friction (COF) between tolerance ring and sleeve was 0.70-0.95 [7]. In case the tolerance ring has material properties following: hardness 400-450 VPN, ultimate tensile strength 1310 MPa, yield strength (0.2% offset) 1170 MPa.

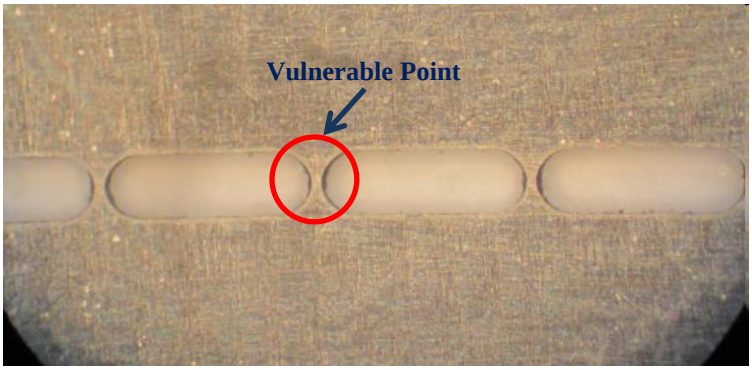

Figure 5: Vulnerable point of the tolerance ring

Table 1: Material properties for finite element analysis

Material Properties	Type of Materials	
	Stainless steel	Aluminum
Elastic modulus, E (MPa)	190,000	71,016
Yield stress, Y (MPa)	206	275
Poisson ratio	0.32	0.33
Mass density (kg/m^3)	7,889	2,700

IV. RESULTS AND DISCUSSIONS

Figure 6 shows the vulnerable points deformation or collapse of the tolerance ring. Red, blue and green point represent the vulnerable point before collapse, top of one after collapse and bottom of one after collapse, respectively. Obviously, the vulnerable points moved from original after apply compression force to the tolerance ring. All points trend to shift in radial trajectory except point A where shift in tangent trajectory. However, moving of the vulnerable points to radial trajectory was required to frictionally engage the tolerance ring and bearing sleeve with an inner surface of an actuator arm. Hence, a space of between ends of the sheet that was formed as the tolerance ring must be reduced. The optimal vulnerable points collapse of the tolerance ring is shown in Figure 7. It reveals that all points have tend to radial trajectory. The frictionally engage the tolerance ring and bearing sleeve with an inner surface of an actuator arm as shown in Figure 8.

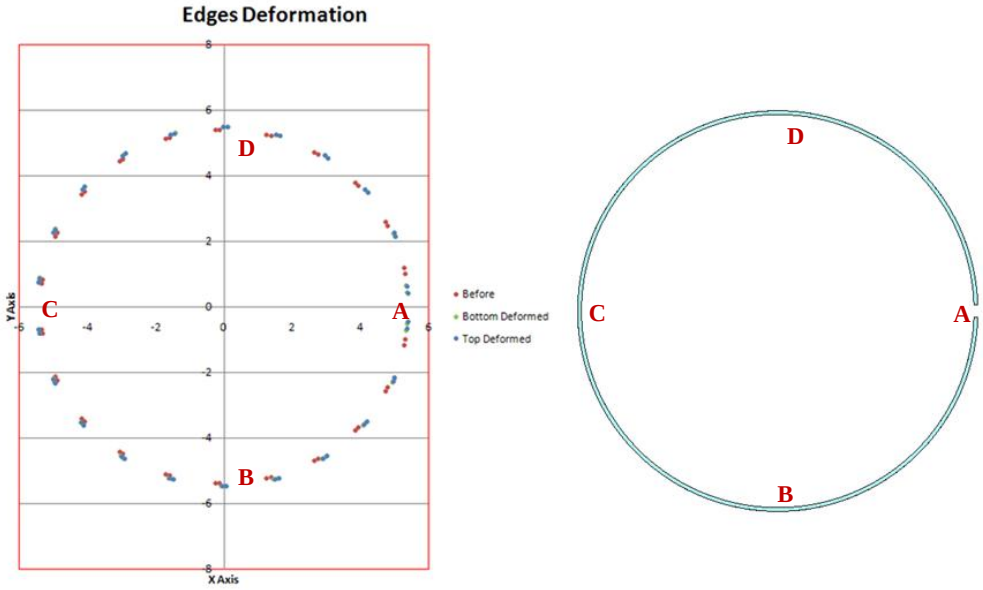

(a) (b)

Figure 6: (a) T-Ring vulnerable points collapse (b) Equivalent diagram

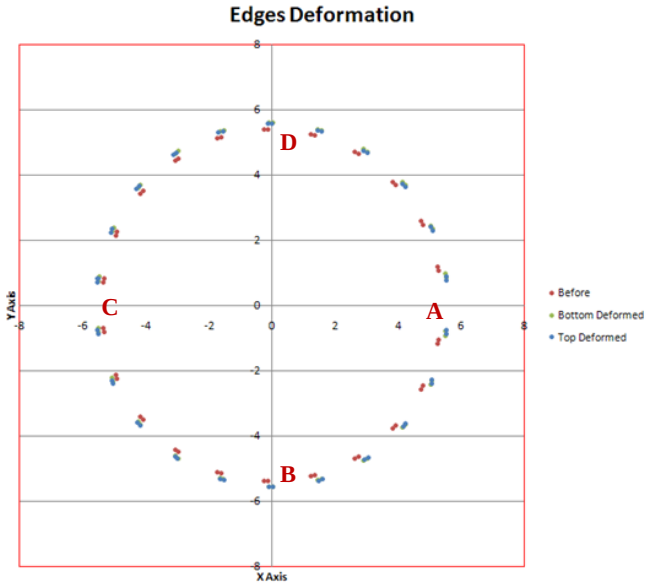

Figure 7: Optimal T-Ring vulnerable points collapse

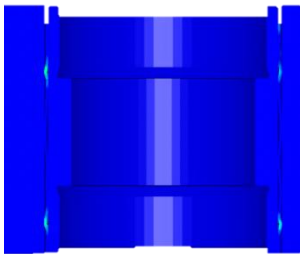

Figure 8: The frictionally engage the tolerance ring and bearing sleeve with an inner surface of an actuator arm

Table 2: Relationship between width of vulnerable point and bearing push out

Vulnerable Point Width (mm)	Bearing Push out (lbf)
0.03	15.1
0.05	37.4
0.07	54.6
0.12	80.3
0.13	70.4

Table 2 shows the relationship between width of vulnerable point of the developed tolerance ring and bearing push out. When vulnerable point width was increased, bearing push out was increased continuously until arrive a measurement and then bearing push out was decreased.

Table 3: Relationship between ratio of space and tolerance ring thickness and collapsed vulnerable point

Space/Ring Thickness Ratio	Collapsed Vulnerable Point (mm)
0	0.11
1	0.19
1.3	0.18
1.5	0.18
1.7	0.18

Table 3 shows the relationship between ratio of a space between the arm actuator and the bearing sleeve and tolerance ring thickness, and collapsed vulnerable point of the developed tolerance ring. The vulnerable point has maximum collapse when space and thickness of the tolerance ring is identical.

V. CONCLUSION

In this paper, finite element models were developed for analysis. All models were meshed with brick element by control the element layer for calculaton of bearing push out. To reduce the particles due to metal scratch in the tolerance ring installation process need to have the optimum vulnerable points. Th tolerance ring is compressed so that it buckles or colapse at predetermined vulnerable points to position the bearing assembly relative to the E-block or actuator arm. The collpse level of vulnerable points designed depend on an axial load or force being applied to the tolerance ring. To have protrusions on the tolerance ring for helping to readily collapse is recommend. Cleanliness can be improved with reducing the movement of components that contact together. From simulation, the tolerance ring is able to move only 2 millimeters that is approximately 97.0% of movement part. Therefore, the developed tolerance ring ensure that the particles are removed from this process.

REFERENCES

[1] R.A. Rongley, "Tolerance rings," United States Patent, Sep. 1, 1981.
[2] Cramer, Jr. et al., "Tolerance ring and shim," United States Patent, May. 9, 1989.
[3] Misso et al., "Top down assembly of a disk drive actuator using a tolerance ring and a post," United States Patent, Sep. 11, 2001.
[4] Macpherson et al., "Cartridge bearing with frictional sleeve," United States Patent, Aug. 12, 2003.
[5] J. Piriyakorn, B. Sujin, "Finite element simulation of a tolerance ring installation process," *The 23rd Conference of the Mechanical Engineering Network of Thailand*, Chiangmai, Thailand, 4-7 November 2009.
[6] Livermore Software Technol. Corp. *LS-Dyna Theory Manual*, Livermore, CA, 2006.
[7] K. Boonlong, "Experiment of friction coefficient between tolerance ring and outer sleeve," Seagate, December 2008.

AUTHORS

First Author – Pattaraweerin Woraratsoontorn, M.Sc (Radiological Science), King Mongkut's Institute of Technology Ladkrabang , oaw2520@hotmail.com.

Second Author – Pitikhate Sooraksa, Ph.D (Electrical Engineering), King Mongkut's Institute of Technology Ladkrabang, kspitikh@kmitl.ac.th

Correspondence Author – Pattaraweerin Woraratsoontorn, oaw2520@hotmail.com, budsapapatn@kmutnb.ac.th, (66)906472455.